NASA
Technical
Paper
2622

September 1986

Secondary-Electron-Emission Losses in Multistage Depressed Collectors and Traveling-Wave-Tube Efficiency Improvements With Carbon Collector Electrode Surfaces

Peter Ramins and
Ben T. Ebihara

NASA

NASA Technical Paper 2622

1986

Secondary-Electron-Emission Losses in Multistage Depressed Collectors and Traveling-Wave-Tube Efficiency Improvements With Carbon Collector Electrode Surfaces

Peter Ramins and
Ben T. Ebihara

Lewis Research Center
Cleveland, Ohio

National Aeronautics
and Space Administration

**Scientific and Technical
Information Branch**

Summary

An experimental program was conducted to investigate secondary-electron-emission losses in multistage depressed collectors (MDC's) and to determine their effects on the overall traveling-wave-tube (TWT) efficiency. Two representative TWT's and several computer-modeled MDC's were used. The experimental techniques provided the measurement of both the TWT overall and the collector efficiencies.

The TWT-MDC performance was optimized and measured over a wide range of operating conditions, with geometrically identical collectors, which utilized different electrode surface materials. Comparisons of the performance of copper electrodes to that of various forms of carbon, including pyrolytic and isotropic graphites, were stressed.

The results indicate that (1) a significant improvement in the TWT overall efficiency was obtained in all cases by the use of carbon, rather than copper electrodes, and (2) that the extent of this efficiency enhancement depended on the characteristics of the TWT, the TWT operating point, the MDC design, and the collector voltages. Ion textured graphite was found to be particularly effective in minimizing the secondary-electron-emission losses. Experimental and analytical results, however, indicate that it is at least as important to provide a maximum amount of electrostatic suppression of secondary electrons by proper MDC design. Such suppression, which is obtained by ensuring that a substantial suppressing electric field exists over the regions of the electrodes where most of the current is incident, was found to be very effective. Experimental results indicate that, with proper MDC design and the use of electrode surfaces with low secondary-electron yield, degradation of the collector efficiency can be limited to a few percent.

Introduction

Modern multistage depressed collectors (MDC's) for microwave tubes provide (by design) electrostatic suppression of low-energy, secondary-electron emission generated on most of the electrode surfaces which receive incident current (refs. 1 to 3). Nevertheless, some backstreaming of secondary electrons is always present. This is due to energetic secondaries, actually elastically and inelastically scattered primaries, and the presence of some incident current on regions of the electrodes where no suppression occurs. Such backstreaming results in degradations of the overall tube and collector efficiencies.

The Lewis Research Center has conducted a largely experimental investigation of the secondary-electron-emission losses in MDC's, in order to quantify such losses and identify ways of minimizing them. In part, traveling-wave tube (TWT) and MDC efficiencies were measured for geometrically identical MDC's by utilizing electrode surfaces with various secondary-electron-emission characteristics. The study compared the TWT overall and collector efficiencies obtained with copper electrodes to those obtained with various carbon forms of low secondary-electron yield. This investigation was part of a joint NASA-USAF program to improve the performance (efficiency) of TWT's for use in communication and electronic countermeasure (ECM) systems. Some limited results of this investigation, obtained with a broad-band TWT of medium electronic efficiency and medium perveance, were reported in references 4 to 6. This paper reports the latest experimental results, as well as some updated results of the earlier studies, including the following:

(1) Evaluation of a particular form of high-purity isotropic graphite as an MDC electrode material, POCO Graphite, Inc., DFP–2

(2) Evaluation of pyrolytic graphite in MDC's, which are designed to collect most of the spent electron beam on the lower secondary-electron-emission yielding C-direction surface (ref. 7)

(3) Evaluation of ion beam texturing and mechanical surface roughening of isotropic graphite as possible techniques for improving the tube and collector performance

(4) Use of a different type of TWT (a design with very high electronic efficiency and perveance) in conjunction with a collector of small size.

The authors wish to express their gratitude to A.N. Curren of the NASA Lewis Research Center for the ion texturing of the pyrolytic graphite and isotropic graphite MDC electrode surfaces.

Symbols

B_z	axial magnetic field, T
f	operating frequency, GHz
I_B	intercepted-beam current, A
I_{en}	current to collector electrode n, A

I_G total body current, including backstreaming from collector, A

I_0 beam current, A

I_s backstreaming current to the TWT body including current to MDC stage (if any) at ground potential, A

P_{body} body power, sum of RF circuit losses and intercepted-beam power in forward direction, W

P_{col} collector power, $V_0 I_0 - P_{RF} - P_{body}$, W

P_{rec} recovered power, $\sum_{n=1}^{4} \left(|V_0| - V_{en}\right) I_{en}$, W

P_{RF} total RF output power, W

P' prime power, $V_0 I_G + \sum_{n=1}^{4} V_{en} I_{en}$, W

V_{en} voltage on collector electrode n, with respect to cathode, V

V_0 cathode potential with respect to ground, V

η_{ckt} circuit efficiency, $\dfrac{P_{RF}}{(P_{RF} + \text{circuit losses})}$

η_{col} collector efficiency, P_{rec}/P_{col}, percent

η_e TWT electronic efficiency, $\dfrac{P_{RF} + (\text{circuit losses})}{V_o I_o}$, percent

η_{ov} TWT overall efficiency, P_{RF}/P', percent

η_{RF} RF efficiency of TWT, $P_{RF}/V_0 I_0$, percent

Secondary-Electron-Emission Losses in Multistage Depressed Collectors

The energies of the electrons in the spent beam of the TWT are determined by the individual TWT parameters and the TWT operating point; V_0, η_e, perveance, and the type and degree of modulation are of particular importance (refs. 8 to 10). Flow diagrams illustrating the distributions of power and electron current are shown in figure 1 for the TWT-MDC system. In the MDC the electrons are slowed down and collected at depressed potentials. The amounts of residual kinetic energy of the electrons and their angles of incidence at the points of impact on the collector electrodes are functions of the entrance conditions, the collector geometry, and the applied potentials. The spectrum of incident electron energies on the various collector electrodes of a given TWT-MDC can be estimated from the considerations outlined by Kosmahl in reference 8.

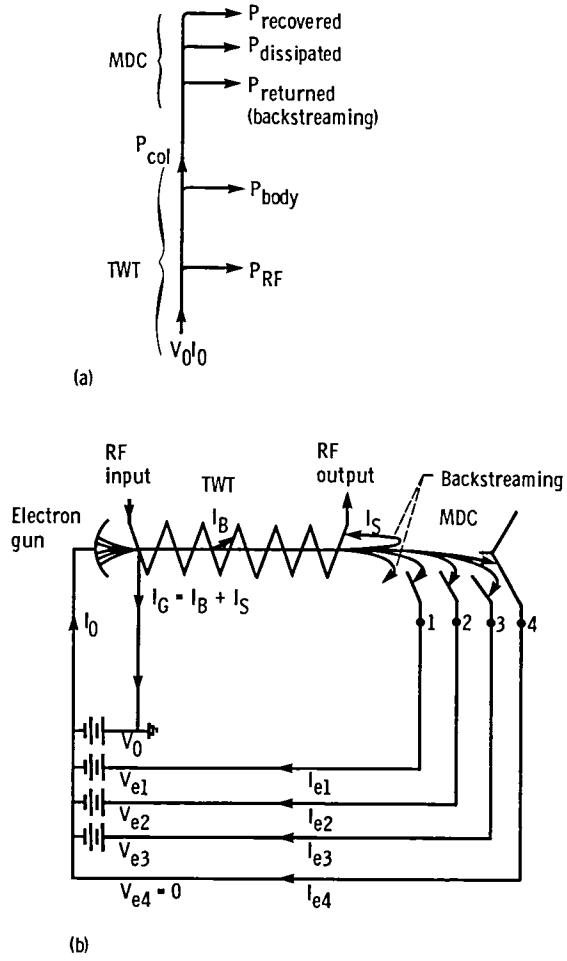

(a) Power flow.
(b) Electron flow.

Figure 1.—Flow diagrams for TWT with four-stage depressed collector.

Electron trajectories in a typical MDC are shown in figure 2 (ref. 11), for two sets of MDC operating voltages. The incident electrons strike the electrode surfaces with a range of energies and angles. Secondary electrons with a range of energies and ejection angles are emitted from the MDC electrode surfaces at the points of impact of the incident electrons. These energy and angular distributions are functions of the incident electron energies and angles, the MDC electrode material, and surface characteristics (refs. 12 and 13).

The secondary-electron trajectories are determined by (1) electric field distribution (including space charge effects) in the MDC and (2) initial velocities of the secondaries. Modern MDC's are designed to suppress most of the low energy (true) secondaries as illustrated in figure 2. Here all but two of the slow (20 eV) secondary electrons are suppressed by the local electric fields. However, the degree of suppression depends on the MDC operating voltages and can be considerably less effective in certain situations. This is illustrated in figure 3 where non-optimum voltages are used and a substantial reduction in the TWT overall efficiency (14 percent in this case) is produced. In the case of MDC electrodes of arbitrary shape and applied potentials (called "Individual-Lens"

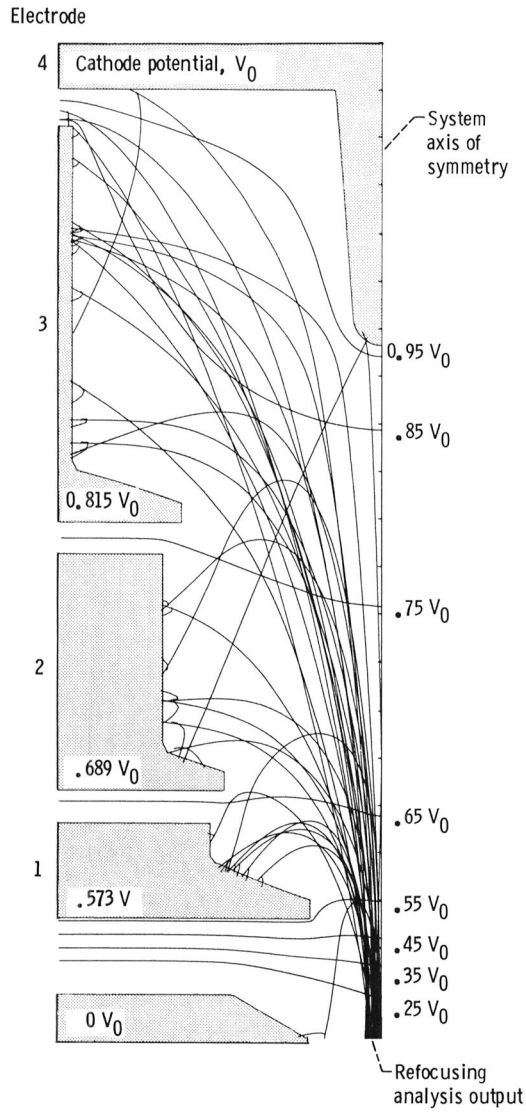

Figure 2.—Charge trajectories for incident primaries and low energy (true) secondaries in a 1.7-cm-diameter four-stage depressed collector operating at optimum voltages. TWT operating at saturation.

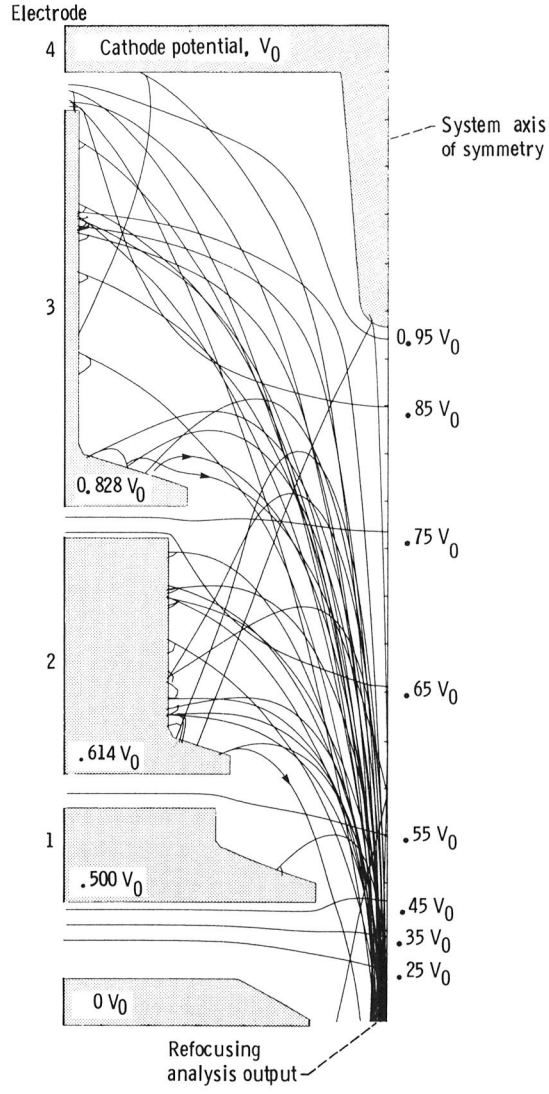

Figure 3.—Charge trajectories for incident primaries and low energy (true) secondaries in a 1.7-cm-diameter four-stage depressed collector operating at non-optimum voltages. TWT operating at saturation.

collector (ILC) by Kosmahl in ref. 10), electrostatic suppression of low energy secondaries from the tops of electrode surfaces cannot be taken for granted; it must be assured by careful design. This is not the case for the "Dispersive-Lens" collectors (DLC) described in reference 10, which provide such suppression automatically.

Furthermore, under some conditions, the incident beam can strike the inner apertures or the bottoms of the electrodes, and the local electric field accelerates the secondaries inward and downward. In the case of the energetic, elastically and inelastically scattered primary electrons, the electrostatic suppression is much less effective at all locations, and a greater probability exists of secondary-electrons backstreaming to less depressed MDC stages or to the TWT body itself (see figure 9 of reference 11). All such backstreaming of secondary electrons results in (1) a reduction of the spent beam power recovered by the collector and (2) reduced TWT overall and collector efficiencies. The magnitude of the losses depends on the following:

(1) TWT parameters
(2) TWT operating point
(3) MDC geometry and voltages
(4) Refocusing system characteristics
(5) MDC electrode material and surface characteristics

There are a number of impediments in the analytical determination of secondary-electron backstreaming losses. First, the energies, angles, and points of impact of the incident electrons may not be known with sufficient accuracy and detail from the computed spent beam energy and collector electrode current distributions (refs. 9 and 11). Secondly, detailed secondary-electron-emission characteristics (the energy and angular distributions as functions of incident energy and angle) have not been available for MDC materials and surface characteristics of current interest. Finally, an accurate computation of the secondary-electron-emission losses may not be cost effective.

An estimate of the secondary-electron backstreaming losses can be made from the measurement of the overall and collector efficiencies of representative TWT and MDC's, each of which utilizes (successively) various MDC-electrode surfaces. However, it is the magnitude of the improvement in the overall TWT efficiency, obtained by utilizing MDC electrodes with reduced secondary-electron-emission characteristics, that is of greatest interest to the TWT designer.

Experimental Program

With the two TWT's and some of the MDC geometric designs described in references 9 and 14, the TWT overall and the MDC efficiencies were measured for a series of collectors of identical geometric design which utilized various electrode surface characteristics (materials and surface topographies). The program stressed a comparison between the performance of TWT-MDC systems with copper collector electrodes (the industry standard) to those with various forms of carbon (in bulk or thin coating form).

In the MDC optimization studies reported in references 9 and 14, the copper collector electrodes were coated with a thin layer of carbon black to reduce the secondary-electron-emission losses. Such a procedure has been found to be highly effective for experimental laboratory MDC's, because a highly reproducible, low-yield coating can be applied to the collector electrodes in a matter of seconds. However, it is not considered suitable for practical MDC's because of the questionable durability and adhesion of the coating under intense electron bombardment. Consequently, a baseline for TWT and MDC performances was subsequently obtained with the carbon-black coating removed from the copper electrodes.

A search for potentially practical MDC electrode materials with low secondary-electron-emission yield characteristics had identified several promising forms of graphite and/or techniques to modify the electrode surface topography to further reduce the secondary-electron emission (refs. 11 and 15 to 17). The TWT and MDC performances were evaluated with a number of these potentially practical, collector-electrode materials by using the same TWT's and identical MDC geometries. This investigation concentrated on a comparison of the collector and TWT overall efficiencies for the various electrode materials; other important issues for practical collector electrodes, such as long-term stability, outgassing characteristics, and fabrication technology, are being addressed in a separate ongoing investigation.

Experimental Arrangement

The TWT and demountable MDC measuring system described in references 4 and 5 were used to optimize and measure the TWT and MDC efficiencies. Because each of the two TWT's had an ultrahigh vacuum (UHV) valve at the end of the refocusing region, the same TWT could be operated with a series of collectors without losing vacuum. (See, for example, figures 4 and 6 of reference 4.) Traveling-wave-tube performance changes from test to test were minimized because no high-temperature TWT bakeout (or removal of the magnets from the Periodic Permanent Magnet (PPM) stack) was required. The TWT RF output power and body power had been measured previously with an undepressed collector (refs. 5 and 14). Consequently, the MDC efficiency, as well as the TWT efficiency, could be measured on subsequent MDC tests as long as the RF performance of the TWT stayed relatively constant. The use of the same TWT (as opposed to the use of a number of TWT's of identical design) was of considerable importance in this study. It had been previously observed that TWT's of identical design can exhibit significantly different $P_{RF}(f)$ and $P_{body}(f)$ characteristics, and thus would make it impossible to resolve the differences in collector efficiency of the order of 1 percent that were obtained by using the same TWT. All but two of the MDC's were demountable. The demountable copper-electrode collectors (with and without the carbon black coating) were individually water cooled and the thermal power dissipated on each was measured. In this way, the average energy of the electrons incident on the MDC electrodes could be estimated in some cases.

The demountable graphite collectors were all radiation cooled. All of the demountable collectors utilized a metallic spike which protruded through the most depressed electrode. The length of the spike could be varied while the TWT was operating. Two of the pyrolytic graphite collectors were conduction-cooled brazed assemblies (ref. 18). The passive support structures and various types of cooling have no bearing on the measured efficiencies, since the important dimensions of the active part of the collector (which influences electron trajectories) were maintained.

The TWT's had a variable refocusing system consisting of two coils. The TWT and MDC performances could be optimized by varying the coil locations and currents, as well as the collector electrode voltages and the length of the spike, as described in reference 4.

Experimental Traveling-Wave Tubes and Multistage Depressed Collectors

Traveling-Wave Tubes

The general characteristics of the two TWT's used in these tests are shown in table I. The very high electronic efficiency and high perveance of VA 101 combine to produce large energy and angular spreads in the spent beam (ref. 19). The range of computed electron energies at the input to the MDC is 2.4 to 7.4 keV. The gridded gun of the TWT introduces additional beam ripple and contributes to the large range of electron angles at the MDC input. The T MEC 103 is a medium electronic efficiency, medium perveance, dual mode

TWT. However, only the low continuous wave (CW) mode was used in this test program with various MDC electrode materials. The computed range of electron energies at the MDC input is 5.2 to 10.2 keV and the range of angles is moderate (ref. 9).

Multistage Depressed Collectors

The general characteristics of the MDC's used in these tests are shown in table II. The approximate MDC geometries are shown in figures 4 to 6. These are reproduced from references 9 and 19 and also show the computed trajectories of typical charges in these collectors. The lines in the solid portions of the electrodes illustrate the arrangement of layers in the pyrolytic graphite versions of these collectors. Following the convention used in reference 7, these layers of graphite will be considered to fall in the *AB*-plane of a rectilinear coordinate system. The *C*-axis (or *C*-direction), which lies along the line of deposition of the pyrolytic graphite, cuts across the exposed *AB*-plane layers of the pyrolytic graphite at the electrode surfaces.

It is apparent that, while MDC 2 uses almost entirely *AB*-plane surfaces to collect incident current, MDC's 3 and 1 use an increasing amount of the lower secondary yield *C*-direction surface.

With the exception of the pyrolytic graphite versions of MDC's 1 and 3, all of the MDC's were demountable and used stainless steel spikes of individually optimized length. The two exceptions utilized fixed-length spikes of molybdenum and isotropic graphite in MDC designs 3 and 1, respectively.

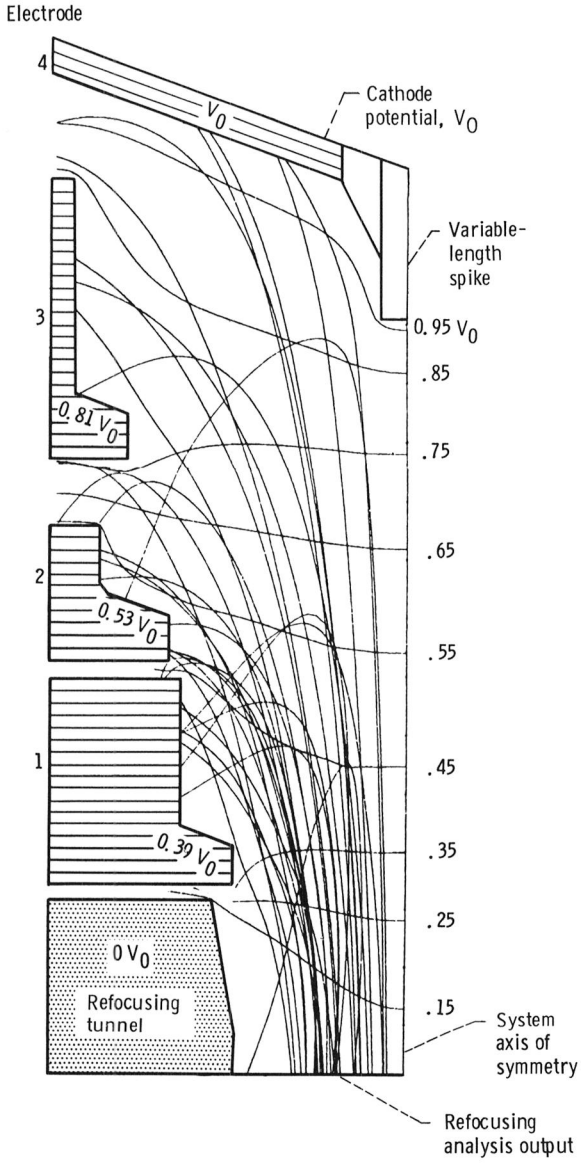

Figure 4.—Geometry of MDC 1 and charge trajectories in collector with TWT operating at saturation. Striated markings symbolize AB-planes of pyrolytic graphite layers. *C*-direction is perpendicular to the *AB*-planes.

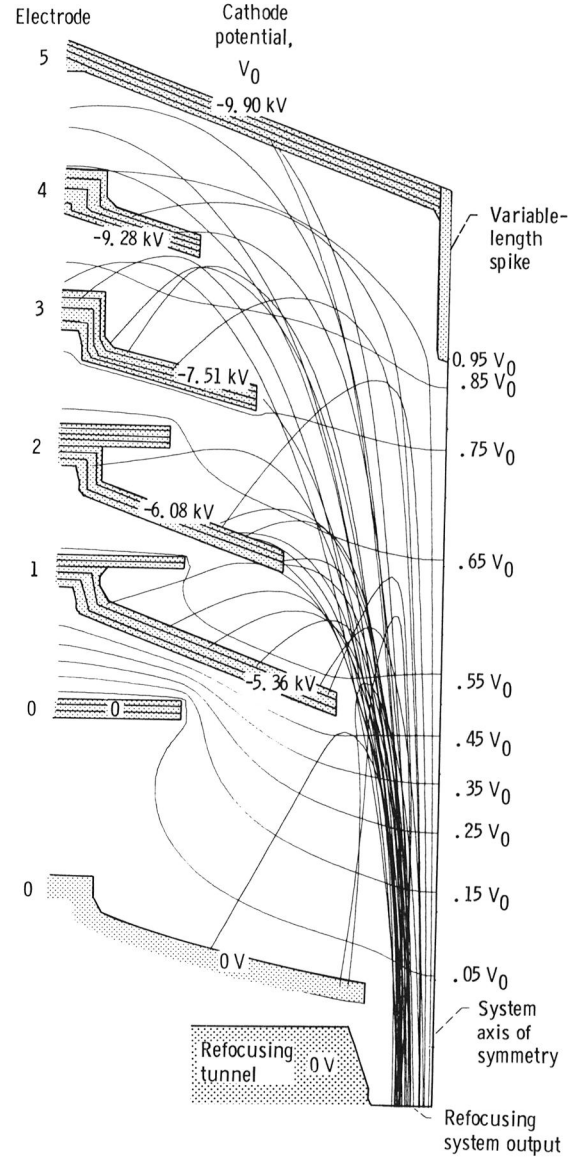

Figure 5.—Geometry of MDC 2 and charge trajectories in collector with TWT operating at saturation in low mode. Striated markings symbolize *AB*-planes of pyrolytic graphite layers. *C*-direction is perpendicular to the *AB*-planes.

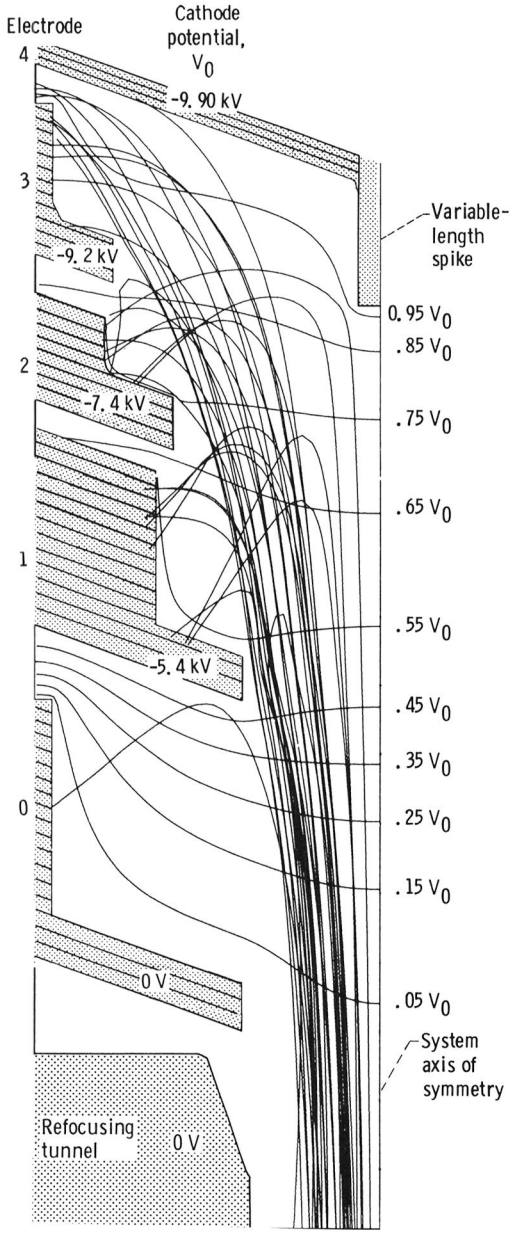

Figure 6.—Geometry of MDC 3 and charge trajectories in collector with TWT operating at saturation in low mode. Striated markings symbolize *AB*-planes of pyrolytic graphite layers. *C*-direction is perpendicular to the *AB*-planes.

Because the thin spike itself is believed to collect little or no current (based on analysis of electron trajectories) the use of various spike materials is believed to have little, if any, effect on the results.

The number of collector stages is defined as the number of distinct voltages, other than ground, needed to operate the MDC. MDC 1 was operated in both three- and four-stage configurations. In the three-stage configuration of MDC 1, electrodes 1 and 2 were operated at the same voltage.

Summary of TWT-MDC Tests and Performance Comparison Cases

The tests performed, the MDC electrode materials evaluated, and the performance comparisons possible are summarized in table III. In the demountable collector tests, where possible, the same set of electrodes and supports were used to eliminate the possibility of performance differences due to any dimensional variations. This was the case in all of the comparisons between copper and carbon black, in the isotropic graphite tests, and the MDC 2 variant tests. The pyrolytic graphite version of MDC 2 is labeled variant because of significant deviations from required dimensions, as discussed later.

Experimental Procedure

Multistage Depressed Collector Performance Comparisons

In comparing TWT and MDC efficiencies obtainable with various MDC electrode materials, a number of different techniques were considered. The tube and collector efficiencies could be obtained and compared for various collector electrode materials utilizing identical MDC geometries and TWT and MDC operating conditions. However, the measured differences in TWT and MDC performance would be of limited value, since their magnitude would depend significantly on how the fixed set of TWT and MDC operating conditions was selected. All MDC's, when operated at maximum efficiency, produce some backstreaming to the TWT body, and the maximum amount of allowable collector depression is sometimes determined by the limits set on the total body current. It has been found that, in general, with electrode materials exhibiting reduced secondary-electron-emission characteristics, the MDC electrodes can be operated at increased levels of depression (and, therefore, higher efficiency) before comparable levels of total body current are reached. Consequently, if the TWT and MDC operating conditions were set up (optimized) for the MDC electrode material with high secondary-electron emission (such as copper), the lower collector depression would not permit the low-yield material to operate at full efficiency and the differences in the efficiencies would be reduced. Conversely, if the TWT and MDC operating conditions were set up for the low-yield electrode material, the higher collector depression would cause excessive backstreaming to the TWT (in some cases exceeding allowable limits on the total body current) and lead to exaggerated performance differences.

In principle, the MDC-electrode geometry should be optimized individually for each distinct MDC-electrode material. This approach, however, was not considered practical for the two following reasons: (1) The analytical design technique available today is not sufficiently refined,

and (2) an individual experimental optimization for each material would require a long program with uncertain results and a considerable risk of TWT performance changes before the program was completed.

References 5 and 20 report that, with a variable spent-beam refocusing system and individual optimization of the operating voltages, collectors of fixed geometric design (MDC 2 and 3) produced very high efficiencies for each of a wide range of TWT applications. Based on these observations, it was decided that the combination of variable refocuser, individual collector-voltage optimization, and spike length optimization (a small geometric change) permitted sufficient flexibility to produce a meaningful comparison of TWT and MDC performance with different MDC-electrode materials.

Efficiency was optimized at a single operating point, rather than as an average over a range of frequencies, to eliminate operator judgement as a signification factor in the results. However, no technique can eliminate operator judgment entirely, since the same or nearly the same optimum MDC efficiency can be obtained with slightly different MDC voltages. These different sets of possible operating voltages can lead to larger differences in MDC efficiency at other frequencies, although such differences are believed to be relatively small.

Performance Optimization Technique

The TWT and MDC performance was individually optimized for each collector electrode material by using the optimization technique described in reference 4. The variables used to optimize the TWT overall and MDC efficiencies were

(1) Individual collector stage voltages
(2) Refocusing coil currents and (over a limited range of variability) the coil positions
(3) Length of the variable spike

The VA 101 TWT and MDC 1 efficiencies were optimized for TWT operation at saturation at the operating frequency (4.75 GHz) that yielded the highest electronic efficiency. Data were then taken at saturation across the operating band of 2.5 to 5.5 GHz at the fixed set of refocuser and MDC operating conditions. In addition, data were obtained below saturation and across the linear range of the TWT (at 4.75 GHz) at the same fixed set of refocuser- and MDC-operating conditions.

The T MEC 103 and MDC 2 efficiencies were optimized for TWT operation at saturation at midband. Data were then taken at saturation across the operating band of 4.8 to 9.6 GHz at the same fixed set of refocuser- and MDC-operating conditions. In addition, data were obtained for the low end of the linear range of the TWT, with the TWT and MDC efficiencies optimized individually at each operating point.

The T MEC 103 and MDC 3 efficiencies were optimized for TWT operation at saturation at the operating frequency (9.2 GHz) yielding the highest electronic efficiency. Three sets of data at cathode currents of 0.38, 0.40, and 0.42A were then taken at saturation across the operating band at this fixed set of refocuser- and MDC-operating conditions. Because RF performance of the TWT across the operating band had changed from the time of the test of MDC 3 with carbon black, the TWT body losses were subsequently remeasured with the TWT operated with the undepressed collector, and used to compute the efficiencies of the pyrolytic graphite version of MDC 3.

RF Test Conditions and Duty Cycle

Filtered input drive at the fundamental frequency was used throughout these tests. Saturation was determined by using an uncalibrated power meter which (with a low pass filter) measured RF power only at the fundamental frequency. However, only the total RF power, which was dissipated in the water-cooled matched load, was measured, and all TWT overall and electronic efficiencies reported here are based on this P_{RF}.

The VA 101 is rated for CW operation. However, to insure that the single tube available would survive the extensive test program, it was operated at a 25 percent duty cycle, with 1.5-msec pulses. The thermal measurements were averages over the pulse time, while the electrical measurements (currents) were instantaneous samples near the end of the pulse. The T MEC 103 was operated in the CW (low) mode for all tests with MDC 2 and for the carbon black version of MDC 3. The pyrolytic graphite version of MDC 3 was tested at a 50 percent duty cycle.

Experimental Results of VA 101 and MDC 1

The TWT performed well for the entire sequence of tests shown in table III. With careful adjustment of the coaxial RF load, optimization of the variable refocusing system, and duplication of previous operating conditions, good repeatability in the TWT performance was obtained from test to test. Consequently, while comparisons to copper are stressed here, the performances of all the MDC-electrode materials can be compared to each other.

Results at Saturation

The RF, TWT overall, and MDC efficiencies as functions of frequency at saturation for copper, carbon black, and pyrolytic graphite are shown in figures 7 and 8 for the four- and three-stage versions of MDC 1, respectively. The TWT overall and MDC efficiencies for copper and isotropic graphite are shown in figures 9 and 10 for the four- and three-stage collectors, respectively. The average TWT and MDC performance across the operating band at saturation for the various MDC-electrode surfaces is summarized in table IV. The relative improvements in the TWT overall and MDC efficiencies of carbon compared with copper electrodes are summarized in table V. The test of a textured carbon on copper MDC reported in reference 21 was part of this test

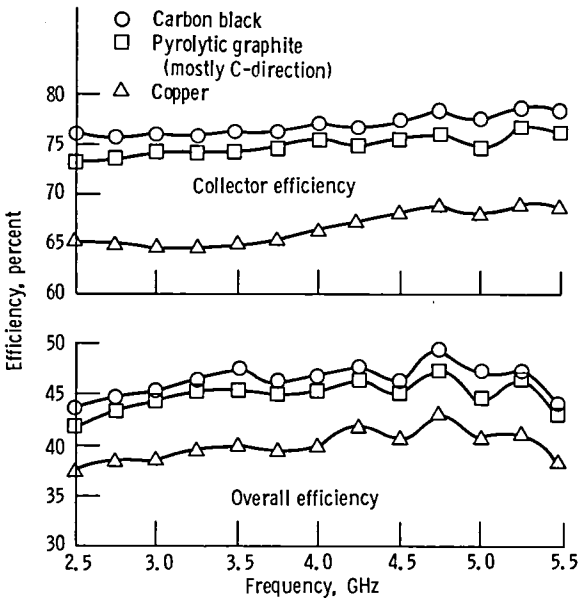

Figure 7.—Collector and TWT overall efficiencies as a function of frequency at saturation for VA 101 and MDC 1 (four-stage).

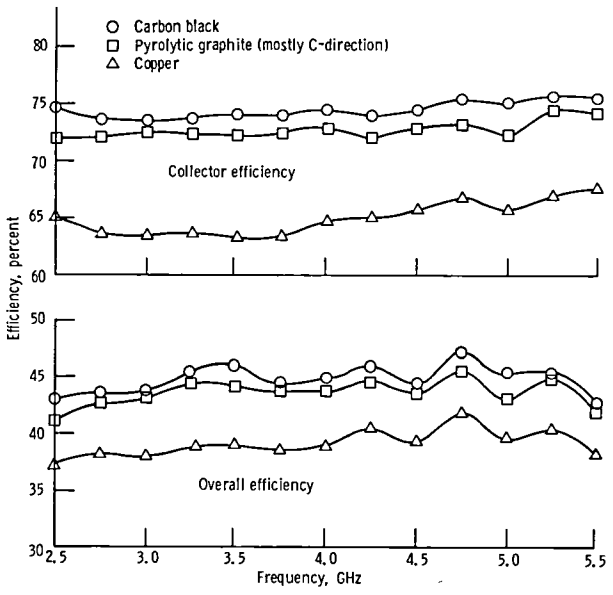

Figure 8.—Collector and TWT overall efficiencies as a function of frequency at saturation for VA 101 and MDC 1 (three-stage).

sequence. The reported average TWT overall and MDC efficiencies were 45.3 and 75.1 percent for the four-stage collector and 44.1 and 73.5 percent for the three-stage collector. These efficiencies compare very favorably to those of the other forms of carbon. The secondary-electron-emission losses in this collector are very large and a significant improvement (10 to 16 percent) in both the TWT overall and MDC efficiencies can be realized by the use of various carbon MDC-electrode surfaces.

In the test involving isotropic graphite, a single set of MDC electrodes was used. Following the test with machined electrode surfaces, all active electrode areas were lightly bead blasted with 50-μm alumina particles. The resulting roughened surface produced a small decrease in the total secondary-electron-emission yield and a modest but noticeable improvement in the TWT overall and collector efficiencies. The subsequent ion beam texturing of the active electrode surfaces (ref. 16) produced a considerably larger improvement in performance. However, as discussed in reference 6 for the case of the textured full-scale, pyrolytic graphite MDC electrodes of complex geometry, electron microscope examination of the textured isotropic-graphite electrode surfaces also indicated less than optimum texturing of large areas of the electrodes, as compared with the surfaces of small flat samples. Consequently, some additional improvements in the efficiencies can be expected as the technique of texturing complex surfaces is perfected.

The pyrolytic graphite MDC used the lower secondary-electron-emission yield *C*-direction surfaces for most of the electrode areas which receive incident current. The exceptions were the flat portions of the tops and bottoms of electrodes 1 to 3 (fig. 4) and all of electrode 4 (exclusive of the spike itself). However, while these areas were nominally *AB*-plane pyrolytic graphite, machining to the required dimensions might well have produced some cutting across overlying *AB*-planes, and thus a mix of *AB*-plane and *C*-direction surfaces would result.

A significant part of the secondary-electron-emission losses in MDC 1 can be attributed to true (low energy) secondaries. Not only is there significant incident current (up to 3.5 percent of I_0) on the conical, most depressed stage, but there are both

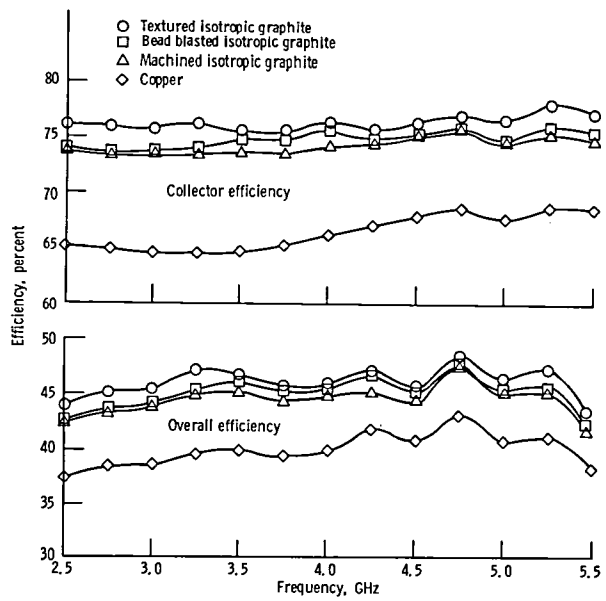

Figure 9.—Collector and TWT overall efficiencies as a function of frequency at saturation for VA 101 and MDC 1 (four-stage).

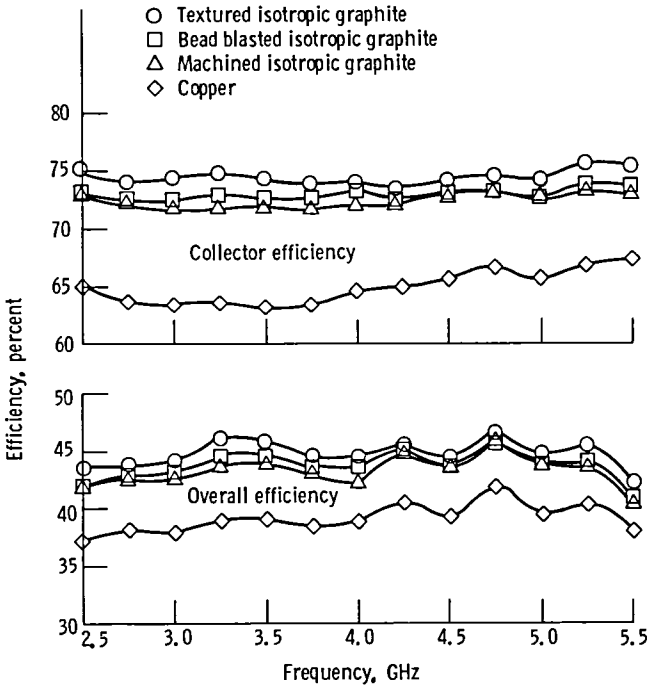

Figure 10.—Collector and TWT overall efficiencies as a function of frequency at saturation for VA 101 and MDC 1 (three-stage).

analytical and experimental indications that the inner edges (apertures) and lower sides of one or more electrodes (where the local electric field accelerates all secondaries downward and/or inward) receive some incident current (fig. 4). Moreover, an examination of the local electric field distribution over the top surfaces of the electrodes has identified several regions (near the apertures of electrodes 1 and 3) where little or no suppression of even low-energy secondary electrons would occur. Some of these effects are consequences of the large range of angles and energies, and of significant space-charge forces at the MDC input due to VA 101. The loss in efficiency attributed to these low energy secondaries is larger over the lower half of the operating band, in part because the incident current on electrode 4 (where all of the secondary electrons are accelerated to less depressed electrodes or to the TWT body) is substantially higher than in the upper part of the operating band (e.g., 23 and 4 mA at 2.75 and 4.75 GHz, respectively).

Since all of the secondary-electron emission from electrode 4 leaves it, the measured values of the net current I_{e4} for the various electrode materials (at similar fixed sets of TWT and MDC operating conditions) can be used to estimate effective total secondary-electron-emission yields (average values for a range of incident electron angles and energies), for those materials. Table VI shows the measured currents and estimated yields for the TWT operating at saturation at 2.75 GHz. The yields were computed with the assumption (ref. 7) that the average yield for carbon black is 0.50 for the range of angles between 45° and 75° (fig. 4) and an average incident energy per electron of about 1 keV (based on the thermal power dissipated on electrode 4).

The MDC operating voltages, which can influence the incident current, were almost identical for carbon black, isotropic graphite, and the carbon on copper collectors, but sufficiently different for the pyrolytic graphite and copper collectors to influence the computed yields somewhat. In general, the computed yields show good correlation with the measurements reported in references 7 and 15 to 17 on small samples. The textured versions of electrode 4 (fig. 4), which is of relatively simple, low-relief shape, exhibited a uniform high quality texture similar to that obtained on small samples; the comments made earlier regarding nonuniformity do not apply here.

The optimized MDC voltages, shown in table VII, are lower for copper than for most forms of carbon. Such reduced voltages have the effect of (1) increasing the suppressing electric field on the tops of electrodes 1 and 3 and (2) increasing the average energy of the incident electrons. The former could result in reduced backstreaming due to slow secondaries. The latter could result in reduced backstreaming of reflected primaries, since the reflected primary yield for copper decreases measurably with increasing incident electron energy, for the typical incident electron energies involved here (ref. 16). A similar explanation may be given for the slightly smaller secondary-electron-emission losses in the three- as compared to four-stage versions of MDC 1 and the surprisingly small improvements in the efficiencies due to the additional stage.

Results Below Saturation

Figures 11 and 12 show the TWT and MDC efficiencies as a function of the RF output power at 4.75 GHz for the four- and three-stage collectors, respectively, for the same fixed sets of refocusing system and MDC operating conditions that were used to obtain the data at saturation. The collector efficiency increases steadily with decreasing RF output power. The relative improvement in collector efficiency of the various forms of carbon compared with copper is relatively constant over the entire range. The relative improvement in the overall efficiency increases steadily as the RF output power and the RF efficiency decrease. For example, at $P_{RF} = 200$ W, the four-stage textured isotropic graphite collector improves the overall efficiency by 33 percent relative to the copper collector. The collector efficiencies at the low end of the linear range and for the DC beam are limited by the voltage applied to electrode 3 (see table VII), which was optimized for operation at saturation.

The collector results obtained with the DC beam can be used to determine (1) the upper limit of the secondary-electron-emission losses in each of the collectors and (2) the lower limit

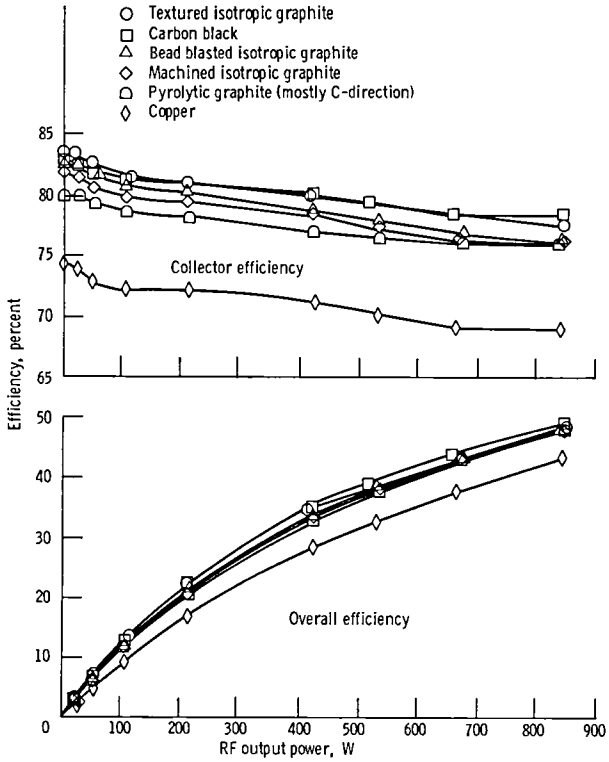

Figure 11.—Collector and TWT overall efficiencies as a function of RF output at 4.75 GHz for VA 101 and MDC 1 (four-stage).

on the combined effectiveness of the electrode surface material/characteristic and the suppressing local electric field in eliminating the backstreaming of secondaries to less depressed stages, for the particular case of the monoenergetic beam striking electrode 3. The former can be obtained from a comparison of $(|V_o| - V_{e3})/V_0$ (the upper limit on the collector efficiency with the DC beam) to the measured collector efficiency; and the latter from a comparison of the measured (net) current, I_{e3}, to the upper limit on the incident current, $I_0 - I_B$. The results are shown in table VIII. In comparing the various materials, it should be noted that the true incident current on electrode 3 (which is influenced by the MDC operating voltages) might be slightly different in each case, and that yields for both true secondary electrons and reflected primary electrons are functions of energy. For this DC beam case, the reduction in MDC efficiency, due to secondary-electron emission, is no more than 1 to 2 percent for carbon electrodes, and no more than 7 percent for the copper electrode. Total backstreaming secondary-electron-emission current from electrode 3 to less depressed potentials was much higher (10 percent) for copper as compared with any of the forms of carbon (less than 4 percent). Losses associated with backstreaming to the TWT body (the worst case) were particularly high for copper. The combination of carbon electrode surfaces and MDC electrical design was very effective in suppressing harmful secondary-electron emission at this particular operating point.

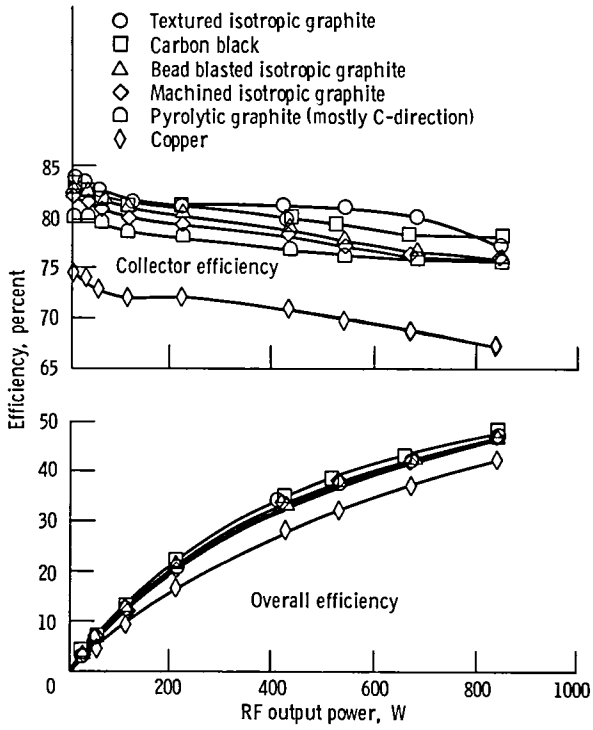

Figure 12.—Collector and TWT overall efficiencies as a function of RF output power at 4.75 GHz for VA 101 and MDC 1 (three-stage).

Experimental Results of T MEC 103 and MDC 2

Table III shows the sequence of tests with carbon black, copper, and pyrolytic graphite electrode surfaces. Following the tests of carbon black and copper versions of MDC 2, an attempt was made to procure geometrically identical pyrolytic graphite electrodes from a manufacturer of that material. This first attempt at fabricating pyrolytic graphite (all *AB*-plane) into complicated shapes resulted in significant deviations from the intended dimensions. These deviations were of the order of about 0.010 in. per part (typically, about 0.050 in. instead of 0.060 in. electrode thickness), but added up in the demountable collector stack. In order to quantify the effect of these dimensional deviations on MDC performance, this collector (labeled MDC 2 variant) was also tested with a coating of carbon black on the pyrolytic graphite electrode surfaces. The carbon black versions of MDC 2 and MDC 2 variant produced slightly different (approx. 1 percent) results. Consequently, in comparing the performance of the copper with the pyrolytic graphite electrodes, the measured results obtained with the copper electrodes were adjusted accordingly at each operating point to compensate for the small geometry differences.

Results at Saturation

Comparisons of the TWT-overall and MDC efficiencies as functions of frequency for both copper and carbon black on

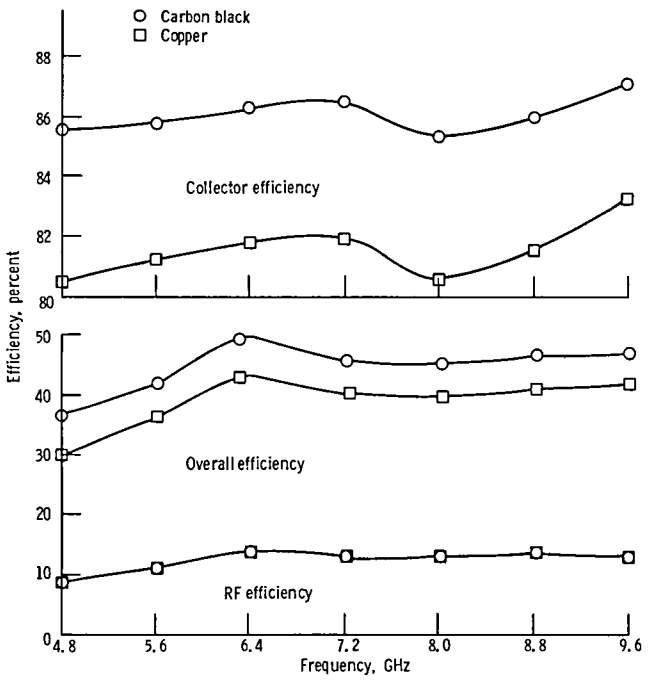

Figure 13.—Collector and TWT overall efficiencies as a function of frequency at saturation for T MEC 103 and MDC 2.

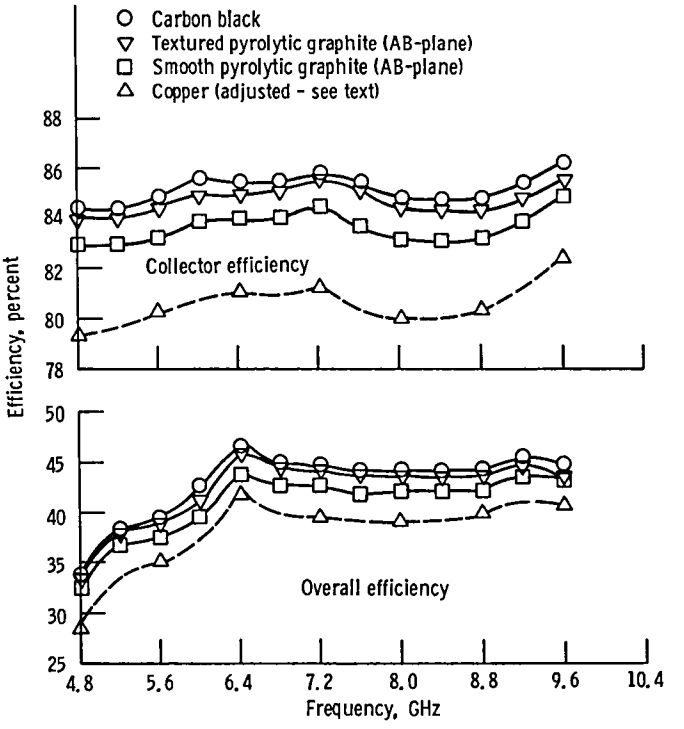

Figure 14.—Collector and TWT overall efficiencies as a function of frequency at saturation for T MEC 103 and MDC 2 variant.

copper are shown in figure 13. Comparisons of TWT overall and MDC efficiencies as functions of frequency for *AB*-plane pyrolytic graphite, ion textured *AB*-plane pyrolytic graphite, and carbon black deposited on the same set of electrodes, as well as the adjusted values for copper are shown in figure 14. The average TWT and MDC performance across the octave operating band at saturation is summarized in table IX. The relative improvements in the TWT overall and MDC efficiencies of the various forms of carbon compared with copper electrodes are summarized in table X.

The magnitude of the secondary-electron-emission losses is smaller in MDC 2 and the relative improvements in collector efficiency due to various forms of carbon as compared to copper electrodes, of 4 to 6 percent, are smaller than in MDC 1. The relative improvements in the TWT overall efficiency of 8 to 14 percent, however, are comparable to those obtained with VA 101. This is a consequence of the characteristics of the relationship between η_{ov} and η_{col} where

$$\eta_{ov} = \frac{\eta_{ckt} \cdot \eta_e}{1 - \eta_{col} + \eta_e \eta_{col}}$$

(See, for example fig. 3 of ref. 4 for typical plots.) At high η_{col}'s a small improvement in η_{col} will produce a much larger relative improvement in η_{ov}. The smaller secondary-emission losses in MDC 2 can probably be attributed largely to the reduction in losses due to low energy (true) secondaries. Analytical results with MDC 2 show that the amount of current incident on the bottoms of the MDC electrodes is minimized, and that better suppression of low energy secondaries, generated on the top surfaces of the electrodes, is provided. This more efficient collector design was made possible by the considerably lower η_e and perveance of T MEC 103, and the attendant reductions in the electron injection angles and in space charge at the input to the collector.

The average incident electron energies on the various electrodes were estimated to be 0.5 to 1.5 keV for MDC 2. These energies are very similar to those for MDC 1 with VA 101. This is in spite of the substantially greater cathode voltage of T MEC 103, and is due to the smaller range of energies in the spent beam of T MEC 103 and the additional (5th) stage of MDC 2.

The pyrolytic graphite version of MDC 2, which utilized the *AB*-plane for all electrode surfaces except the inner apertures, produced a smaller relative efficiency improvement than did the pyrolytic graphite version of MDC 1, which utilized mostly *C*-direction electrode surfaces. This is consistent with the results of reference 7, where the total secondary yield and the reflected primary yield index were found to be substantially higher for the *AB*-plane as compared to the *C*-direction surfaces.

In the case of the textured pyrolytic graphite electrodes, as noted in reference 6, electron microscope examination of the surfaces indicated a less than optimum texturing of large areas of the electrodes as compared with the surfaces of small flat samples. Consequently, some additional improvements in the efficiencies might be expected as the technique of texturing complex surfaces is perfected.

As discussed above, the measured values of current to the most depressed stage (I_{e5}) can be used to estimate the effective, total secondary-electron-emission yield of the electrode surfaces of the various versions of MDC 2. The results are shown in table XI for the TWT operating at saturation at 4.8 GHz. The yields were computed by using the assumption that the average yield of carbon black is 0.60 (ref. 7) at the very large angles of incidence (near grazing) as suggested by computed trajectories. In general, the computed yields show good correlation with measurements reported in references 7 and 16 on small samples. In the case of the textured surface of electrode 5, the electron microscope examination had showed a fairly uniform, high quality texturing on this relatively simple electrode shape.

The optimized values of $(|V_o|-V_{e4})$ for the carbon electrodes were 3 to 4 percent higher than for copper. The other collector voltages, however, showed no consistent pattern.

Results in TWT Linear Range

The MDC and overall TWT efficiencies as a function of RF efficiency are shown in figure 15. The points at the highest RF efficiency shown (6.6 percent) are 3 dB below saturation. The MDC performance was individually optimized at each TWT operating point, for each MDC-electrode material. The relative differences in MDC efficiency narrow somewhat for operation at increasingly lower levels of RF efficiency. The relative overall TWT efficiencies, however, remain relatively constant. For example, the relative improvement in MDC efficiency for carbon black relative to copper drops from about 4.9 to 2.8 percent over the range shown, while the relative improvement in the overall TWT efficiency remains at about 25 percent.

For operation of T MEC 103 over most of its linear range, the average energies of the incident electrons are near those which yield the highest total secondary-electron-emission yield for all of the materials tested. In the case of all forms of carbon, the reflected primary electron index is also near maximum. (See, e.g., refs. 7 and 16.) Nevertheless, the losses due to backstreaming secondaries are very low under some conditions. The upper limits on the MDC efficiency (determined by V_{e4}, as discussed above) and the measured MDC efficiencies for the case of the DC beam are shown and compared in table XII. It is evident that, for these cases of low energies of incidence, the total secondary-electron-backstreaming losses are no more than a few percent, even for the copper electrodes. This is caused by both a combination of lower secondary-electron yields at these low energies of

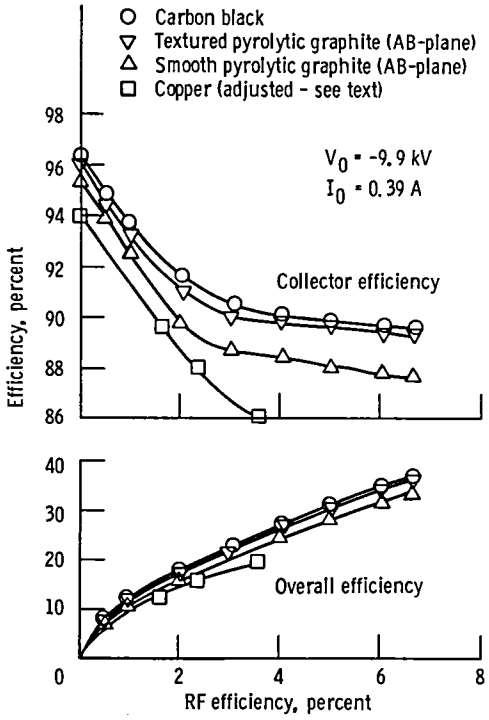

Figure 15.—Collector and TWT overall efficiencies as a function of RF efficiency at 8.4 GHz for T MEC 103 and MDC 2. (Individually optimized at each operating point.)

incidence and the effective suppression of secondaries by the electric fields in the MDC.

The very high MDC efficiencies, of 94.7 to 97.1 percent, obtained with the DC beam confirm that the secondary losses are small. The sum of secondary losses and MDC sorting losses (excess energy needed to reach a given electrode due to radial velocity components) is no higher than 2.9 to 5.3 percent for the various electrode surfaces tested. In this instance, the reductions in MDC efficiency due to the finite number of stages do not apply.

The very high collector efficiencies of 86 to 87 percent for MDC 2 with TWT operation at saturation imply low secondary-emission losses for this case as well. Application of the method outlined by Kosmahl in reference 8 to estimate the MDC efficiency without any secondary-electron-emission losses, for a TWT of this perveance and electronic efficiency, yields results very close to those measured.

Experimental Results of T MEC 103 and MDC 3

The test results of the demountable carbon black on a copper collector are reported in reference 20. By the time the pyrolytic graphite version of this collector (consisting of a mix of *AB*-plane and *C*-direction surfaces) was tested, the performance of the TWT had changed slightly. An attempt was made to

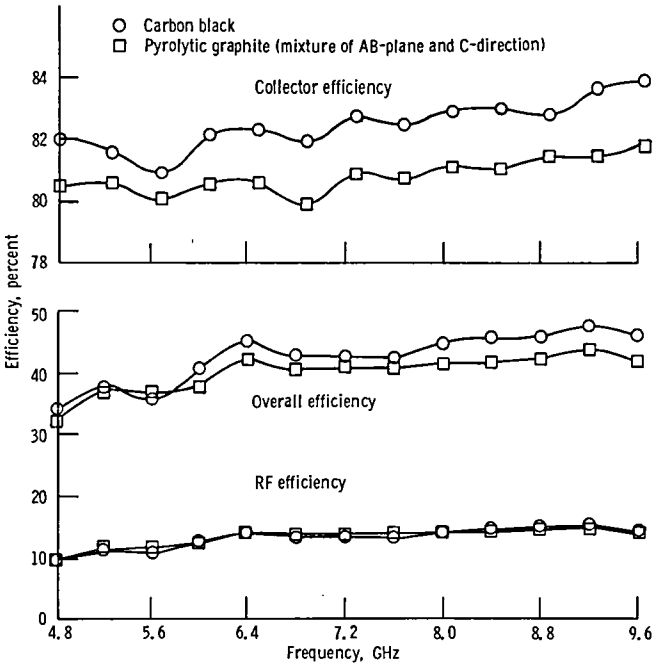

Figure 16.—Collector, TWT overall, and RF efficiencies as a function of frequency at saturation for T MEC 103 and MDC 3 (I_0 = 0.42A).

restore the previous performance by adjusting the magnetic focusing field of the TWT. This attempt was only partially successful; the previous average RF-output efficiency across the operating band was duplicated, but RF-outout power as a function of frequency showed small deviations from the earlier test. After the test completion of the pyrolytic graphite MDC, the TWT performance and total body power were remeasured across the operating band by using an undepressed MDC to collect the spent beam. These new values of the TWT body losses were slightly higher than measured previously. Consequently, while the MDC efficiencies could be properly computed and compared to the earlier test, the resulting differences in the overall TWT efficiencies were slightly exaggerated. Therefore, the overall TWT efficiencies obtained with the pyrolytic graphite collector were adjusted slightly (a fraction of a percent) so that they could be compared to earlier results on an equal basis.

TWT and MDC performances were evaluated at saturation (across the operating bandwidth) at three levels of cathode current. The MDC, TWT overall, and RF efficiencies as a function of frequency for I_0 = 0.42A are shown in figure 16. Similar results were obtained at cathode currents of 0.38 and 0.40 A. The results are summarized in table XIII.

Results of Miscellaneous Tests

Three models of the TWT described in reference 11 (S/N 202 to S/N 204) were tested with pyrolytic graphite (mostly C-direction), textured pyrolytic graphite, and isotropic graphite versions of the 1.7-cm-diameter four-stage MDC shown in figure 2. While very significant individual differences in the $P_{RF}(f)$ prevented meaningful performance comparisons under RF operating conditions, the operation of these devices with a DC beam provides an interesting evaluation of the effectiveness of the secondary-suppression techniques described here.

The MDC performance analyses for the three electrode surfaces with the DC beam are shown in table XIV. The MDC operating voltages were optimized for broadband operation at saturation. For this MDC design and 2.1 to 2.5 keV electrons, approximately 99 percent of the incident current remains on electrode 3, and the loss in η_{col} caused by secondary electron emission is a small fraction of 1 percent.

The MDC performance analyses for the three electrode surfaces with the DC beam are shown in table XIV. The MDC operating voltages were optimized for broadband operation at saturation. For this MDC design and 2.1 to 2.5 keV electrons, approximately 99 percent of the incident current remains on electrode 3, and the loss in η_{col} caused by secondary electron emission is a small fraction of 1 percent.

Reducing Secondary-Electron-Emission Losses in Multistage Depressed Collectors

A number of potential sources of secondary-electron-emission losses have been identified. These include the following:

(1) An improper electric field distribution in the collector, where the local field over regions of the tops of electrodes either fails to suppress low-energy secondary electrons or actually accelerates them away from the electrode surfaces

(2) The presence of incident current, possibly at very large angles of incidence, on the bottom of the most depressed stage

(3) The presence of incident current on the bottoms or the inner apertures of one or more electrodes

(4) Use of electrode surfaces or materials with high secondary-electron yield

The first situation can be largely avoided by a careful computer-aided MDC design, where representative secondary-electron-emission current is injected back into the collector (ref. 11) and/or the electric field distribution over the top surfaces of the electrodes is examined for a range of MDC operating voltages. Performing such MDC analysis, and making sure suppression of low energy secondaries is maintained, is useful because the computed spent-beam-energy distribution is only approximate (as discussed in refs. 9 and 11) and the optimum experimental collector voltages could be somewhat different from the optimum computed values.

Losses due to backstreaming secondaries from the most depressed stage can be reduced by designing the collector such

that the secondaries are collected on a highly depressed adjacent stage. (e.g., see MDC 2) or, in the case of electrode surfaces with an effective yield greater than unity, the current incident on the electrode is minimized.

The situation of significant incident current on the bottoms or inner apertures of the other electrodes can probably be largely avoided by careful computer-aided MDC design for most applications of medium electronic efficiency and medium perveance TWT's (refs. 9 and 11). For the case of high electronic efficiency and high perveance TWT's, however, this situation may lead to large losses. Beam collimation and dilution of space charge by means of controlled beam expansion and refocusing may be effective in some cases. In the case of VA 101 and MDC 1, this approach was only partially successful because of limits placed on collector size. Here the beam size at the MDC entrance was half the size of the collector diameter, deviating significantly from the point source ideal discussed in reference 10.

The use of carbon on the electrode surfaces can lead to significant improvements in the overall TWT efficiency. In the case of pyrolytic graphite, maximum use should be made of the lower yield *C*-direction surface in locations which receive significant incident current. Mechanical roughening on the surface can produce limited improvements in some cases, for example, bead blasting of isotropic graphite. The creation of a textured carbon surface on isotropic graphite, pyrolytic graphite, or copper electrode substrates can lead to significant reductions in secondary-electron-emission losses and improvements in overall TWT efficiency, especially when techniques for generating such surfaces on complex electrode shapes are perfected.

Concluding Remarks

The complicated phenomenon of backstreaming secondary-electron emission from MDC electrodes and the attendant degradations in the TWT overall and MDC efficiencies is influenced by the TWT parameters and operating point, as well as the MDC design, electrode surface characteristics, and operating voltages. The results of this investigation indicate that, while the relative MDC efficiency varied considerably, a very significant improvement in the TWT overall efficiency was obtained in all cases by the use of carbon rather than copper collector electrode surfaces. Ion textured carbon was found to be particularly effective in minimizing the secondary-electron-emission losses. Additional efficiency improvements are possible when the technique of uniform high-quality texturing of complex electrode shapes is perfected.

Because of the number of different cases examined (TWT's, MDC's, and operating points), the wide range of incident electron energies (from a few hundred to a few thousand electronvolts), and angles covered (from normal to near grazing), the results have some applicability for most TWT's. In the case of tubes with very low (< 2 to 3 kV) or very high (> 20 kV) cathode voltages, however, the losses (and improvement in efficiency with carbon) might be significantly smaller. For the case of collector designs which do not provide effective electrostatic suppression of low-energy secondary electrons, the backstreaming secondary-electron-emission losses could be considerably higher. An approximate correlation was found to exist between the measured collector performance and secondary-electron-yield measurements on small samples (allowing for nonuniformities in the texturing of the MDC-electrode surfaces).

The experimental results indicated that, with proper MDC design and the use of electrode surfaces with low secondary-electron yield, degradations in MDC efficiency can be limited to a few percent for some operating conditions. To obtain a better estimate of the magnitude of the losses under a wide range of operating conditions, however, the contribution of the backstreaming elastically and inelastically scattered primaries to the total losses must be clarified. The lack of data on the energy and angular distributions of these energetic secondaries, for the various electrode surfaces of interest, has prevented an analytical investigation of these losses.

This investigation concentrated on secondary-electron-emission losses in MDC's and the improvements in efficiency with carbon electrodes. Issues such as the long-term stability of the carbon surfaces and the outgassing performance are being addressed in a separate investigation, some early results of which are reported in reference 11.

National Aeronautics and Space Administration
Lewis Research Center
Cleveland, Ohio, May 27, 1986

References

1. Sauseng, O.G.; Basiulis, A.; and Tammaru, I.: Analytical Study Program to Develop the Theoretical Design of Traveling-Wave Tubes. (HAC-EDD-W-2646, Hughes Aircraft Co.; NASA Contract NAS3-9719) NASA CR-72450, 1968.
2. Branch, G.M.; and Mihran, T.G.: Analytical Designs of a Space-Borne Magnetically-Focused Klystron Amplifier. NASA CR-72461, 1968.
3. Kosmahl, H.G.: A Novel, Axisymmetric, Electrostatic Collector for Linear Beam Microwave Tubes. NASA TN D-6093, 1971.
4. Kosmahl, H.G.; and Ramins, P.: Small-Size 81 to 83.5-Percent Efficient 2- and 4-Stage Depressed Collectors for Octave-Bandwidth High-Performance TWT's. IEEE Trans. Electron, Devices, vol. ED-24, no. 1, Jan. 1977, pp. 36-44.
5. Ramins, P.; and Fox, T.A.: Multistage Depressed Collector with Efficiency of 90 to 94 Percent for Operation of a Dual-Mode Traveling-Wave Tube in the Linear Region, NASA TP-1670, 1980.
6. Curren, A.N.; and Fox, T.A.: Traveling-Wave Tube Efficiency Improvement with Textured Pyrolytic Graphite Multistage Depressed Collector Electrodes. IEEE Electron Device Lett., vol. EDL-2, no. 10, Oct. 1981, pp. 252-254.

7. Curren, A.N.; and Jensen, K.A.: Beam Impingement Angle Effects on Secondary Electron Emission Characteristics of Textured Pyrolytic Graphite. NASA TP-2285, 1984.
8. Kosmahl, H.G.: How to Quickly Predict the Overall TWT and the Multistage Depressed Collector Efficiency. IEEE Trans. Electron Devices, vol. ED-27, no. 3, Mar. 1980, pp. 526-529.
9. Dayton, J.A., Jr., et al.: Experimental Verification of a Computational Procedure for the Design of TWT-Refocuser-MDC Systems. IEEE Trans. Electron Devices, vol. ED-28, no. 12, Dec. 1981, pp. 1480-1489.
10. Kosmahl, H.G.: Modern Multistage Depressed Collectors-A Review. Proc. IEEE, vol. 70, no. 11, Nov. 1982, pp. 1325-1334.
11. Ramins, P., et al.: Verification of Computer-Aided Designs of Traveling-Wave Tubes Utilizing Novel Dynamic Refocusers and Graphite Electrodes for the Multistage Depressed Collector, NASA TP-2524, 1985.
12. Gibbons, D.J.: Secondary Electron Emission. Handbook of Vacuum Physics, vol. 2, part 3, A.H. Beck, ed., Pergamon Press, 1966, pp. 301-395.
13. Kohl, W.H.: Handbook of Materials and Techniques for Vacuum Devices. Reinhold, 1967.
14. Ramins, P.: Performance of Computer Designed Small-Size Multistage Depressed Collectors for a High-Perveance Traveling Wave Tube. NASA TP-2248, 1984.
15. Forman, R.: Secondary-Electron-Emission Properties of Conducting Surfaces with Application to Multistage Depressed Collectors for Microwave Amplifiers. NASA TP-1097, 1977.
16. Curren, A.N.; and Jensen, K.A.: Secondary Electron Emission Characteristics of Ion-Textured Copper and High-Purity Isotropic Graphite Surfaces. NASA TP-2342, 1984.
17. Curren, A. N.; and Jensen, K.A.: Textured Carbon on Copper: A Novel Surface With Extremely Low Secondary Electron Emission Characteristics, NASA TP-2543, Dec., 1985.
18. Ebihara, B.T.: Multistage Spent Particle Collector and Method for Making Same. U.S. Patent 4,527,092, July 2, 1985.
19. Dayton, J.A., Jr.; Kosmahl, H.G.; and Ramins, P.: Experimental Verification of the Multistage Depressed Collector Design Procedure For a High Perveance, Helix-Type, Traveling Wave Tube. NASA TP-2162, 1983.
20. Ramins, P.; and Fox, T.A.: Performance of Computer-Designed Small-Sized Four-Stage Depressed Collector for Operation of Dual-Mode Traveling Wave Tube, NASA TP-1832, 1981.
21. Curren, A.N.; and Ramins, P.: TWT Efficiency Enhancement with Textured Carbon Surfaces on Copper MDC Electrodes. Presented at the International Electron Devices Meeting, Washington, D.C., Dec. 1-4, 1985.

TABLE I.–GENERAL TRAVELING-WAVE-TUBE CHARACTERISTICS

TWT model	Varian 6336 A1	Teledyne MEC MTZ-7000
Serial number	101 R1	103
Designation	VA 101	T MEC 103
Frequency, GHz	2.5 to 5.5	4.8 to 9.6
Cathode voltage, kV	−6.2	−9.9
Cathode current, A	.60	.38 to .42
Perveance, $A/V^{3/2}$	1.23×10^{-6}	$.39$ to $.43\times10^{-6}$
η_e, percent	26 max	16 max
Focusing	PPM	PPM
Duty cycle, percent	[a]25	100

[a]Nominally CW, limited to 25 percent during these tests.

TABLE II.–GENERAL MULTISTAGE DEPRESSED COLLECTOR CHARACTERISTICS

MDC designation	MDC 1	MDC 2	MDC 3
Applicable TWT	VA 101	T MEC 103	T MEC 103
Number of stages	4 or 3	5	4
Active inner diameter, cm	2.4	5.1	2.4
Active height, cm	3.2	7	3.8
Geometry	(a)	(b)	(c)
Typical MDC efficiency	Medium	Very high	High

[a]See fig. 4.

[b]See fig. 5.

[c]See fig. 6.

TABLE III.–SUMMARY OF TWT-MDC TESTS, ELECTRODE MATERIALS, AND ELECTRODE SURFACE TOPOGRAPHIES

MDC electrode material	Electrode surface characteristics or coating
VA 101 and MDC 1 (four- and three-stage)	
Copper	Bead blasted (for cleaning purposes)
Isotropic graphite	Carbon black Machined Bead blasted (for roughening purposes)
Pyrolytic graphite	Textured Machined (mostly *C*-direction)
T MEC 103 and MDC 2	
Copper	Carbon black Bead blasted (for cleaning purposes)
T MEC 103 and MDC 2 variant	
Pyrolytic graphite	*AB*-plane Textured *AB*-plane Carbon black
T MEC 103 and MDC 3	
Copper Pyrolytic graphite	Carbon black Mixture of *AB*-plane and *C*-direction

TABLE IV.–SUMMARY OF AVERAGE TWT VA 101 AND MDC 1 PERFORMANCE ACROSS 2.5- TO 5.5-GHz OPERATING BAND AT SATURATION

MDC electrode characteristics	Four-stage MDC			Three-stage MDC		
	η_{RF}	η_{ov}	η_{col}	η_{RF}	η_{ov}	η_{col}
Carbon black	21.1	46.2	76.7	21.1	44.7	74.4
Textured isotropic graphite	↓	46.0	76.4	↓	44.7	74.5
Bead-blasted isotropic graphite	↓	45.0	74.9	↓	43.7	73.0
Pyrolytic graphite (mostly *C*-direction)	↓	44.9	74.8	↓	43.5	72.7
Machined isotropic graphite	↓	44.5	74.3	21.0	43.2	72.4
Copper	↓	39.9	66.5	21.1	39.1	64.9

TABLE V.–SUMMARY OF TWT OVERALL AND MDC EFFICIENCY IMPROVEMENTS FOR CARBON COMPARED WITH COPPER MDC ELECTRODE SURFACES FOR VA 101 AND MDC 1

MDC electrode characteristics	Four-stage MDC		Three-stage MDC	
	TWT overall efficiency improvement relative to copper, percent	MDC efficiency improvement relative to copper, percent	TWT overall efficiency improvement relative to copper, percent	MDC efficiency improvement relative to copper, percent
Carbon black	15.9	15.3	14.3	14.6
Textured isotropic graphite	15.2	14.9	14.5	14.8
Bead blasted isotropic graphite	12.7	12.6	11.7	12.4
Pyrolytic graphite (mostly *C*-direction)	12.5	12.4	11.4	12.0
Machined isotropic graphite	11.5	11.6	10.4	11.5

TABLE VI.–MEASURED CURRENT AND COMPUTED AVERAGE TOTAL SECONDARY-ELECTRON YIELD OF ELECTRODE 4

[VA 101 TWT and three-stage MDC 1 operated at 2.75 GHz at saturation.]

MDC electrode characteristics	I_{e4}, mA	Average total yield
Carbon black	11.4	[a]0.50
Textured isotropic graphite	14.5	.36
Bead blasted isotropic graphite	9.6	.58
Machined isotropic graphite	8.6	.62
Pyrolytic graphite (AB-plane)	4.4	.8
Copper	−17.7	1.8
Textured carbon on copper	13.7	.40

[a]Assumed value, based on ref. 7.

TABLE VII.–SUMMARY OF OPTIMIZED VOLTAGES OF FOUR-STAGE MDC 1 WITH VA 101 OPERATING AT SATURATION

MDC electrode surface characteristics	Optimized voltage, normalized to V_0, $\frac{(\lvert V_o\rvert - V_{en})}{V_0}$			
	Electrode 1	Electrode 2	Electrode 3	Electrode 4
Carbon black	0.43	0.52	0.85	1.0
Textured isotropic graphite	.43	.51	.84	
Bead blasted isotropic graphite	.43	.52	.84	
Machined isotropic graphite	.42	.51	.84	
Pyrolytic graphite (mostly *C*-direction)	.43	.51	.81	
Copper	.41	.47	.80	

TABLE VIII.–COLLECTOR PERFORMANCE ANALYSIS WITH DC BEAM FOR VA 101 TWT AND MDC 1

(a) Four-stage collector

Electrode surface characteristics	η_{col} (limit), percent	η_{col} (meas.), percent	$\frac{\eta_{col}(\text{meas.})}{\eta_{col}(\text{limit})} \times 100$, percent	Incident electron energy, eV	$\frac{I_{e3}}{(I_0 - I_B)} \times 100$, percent	$\frac{I_s}{I_0} \times 100$, percent
Carbon black	84.8	82.9	97.7	940	96.0	0.6
Textured isotropic graphite	84.4	83.6	99.1	970	97.9	.0
Bead blasted isotropic graphite	83.9	82.6	98.5	1000	96.9	.6
Machined isotropic graphite	83.9	81.9	97.7	1000	96.0	1.0
Pyrolytic graphite (mostly C-direction)	80.8	79.9	98.9	1190	97.5	.1
Copper	79.7	74.3	93.2	1260	90.2	4.3

(b) Three-stage collector

Carbon black	84.2	81.8	97.2	980	95.7	1.1
Textured isotropic graphite	83.2	82.3	99.0	1040	97.6	.0
Bead blasted isotropic graphite	82.9	81.5	98.3	1060	97.0	.4
Machined isotropic graphite	82.9	80.8	97.4	1060	96.0	1.3
Pyrolytic graphite (mostly *C*-direction)	79.0	77.9	98.7	1310	97.3	.2
Copper	79.5	72.8	91.6	1270	88.0	5.7

TABLE IX.–SUMMARY OF AVERAGE TWT-T MEC 103 AND MDC 2 PERFORMANCE AT SATURATION ACROSS 4.8- TO 9.6- GHz OPERATING BAND

(a) T MEC 103 AND MDC 2

Electrode surface characteristics	η_{RF}, percent	η_{ov}, percent	η_{col}, percent
Copper	12.0	38.5	81.5
Carbon black	12.0	44.4	86.0

(b) T MEC 103 and MDC 2 variant

Copper (adjusted data)	12.0	37.6	80.6
Pyrolytic graphite (*AB*-plane)	11.9	40.7	83.6
Textured pyrolytic graphite (*AB*-plane)	11.9	42.1	84.7
Carbon black	11.9	42.8	85.1

TABLE X.–SUMMARY OF TWT OVERALL AND MDC EFFICIENCY IMPROVEMENTS FOR CARBON COMPARED WITH COPPER MDC ELECTRODE SURFACES FOR T MEC 103 AND MDC 2 VARIANT

MDC electrode characteristics	TWT overall efficiency improvement relative to copper, percent	MDC efficiency improvement relative to copper, percent
Carbon black	13.6	5.6
Textured pyroltyic graphite (*AB*-plane)	11.7	5.0
Pyrolytic graphite (*AB*-plane)	8.2	3.7

TABLE XI.—MEASURED CURRENT AND COMPUTED AVERAGE TOTAL SECONDARY-ELECTRON YIELD OF ELECTRODE 5 OF MDC 2 AND T MEC 103 TWT OPERATING AT SATURATION AT 4.8 GHz

Collector electrode characteristics	I_{e5}, mA	Average total yield
Carbon black on copper	6.4	[a]0.60
Carbon black on pyrolytic graphite	6.6	.59
Pyrolytic graphite (*AB*-plane)	−.1	1.05
Textured pyrolytic graphite (*AB*-plane)	10.6	.34
Copper	−8.6	1.5

[a]Assumed value based on ref. 6, for very large angles of incidence.

TABLE XII.—COLLECTOR PERFORMANCE ANALYSIS WITH DC BEAM FOR T MEC 103 AND MDC 2

Electrode surface characteristics	η_{col} (limit), percent	η_{col} (meas.), percent	$\frac{\eta_{col}(\text{meas.})}{\eta_{col}(\text{limit})} \times 100$, percent	Incident electron energy of electrode 5, eV
Carbon black on copper	98.4	97.1	98.7	130
Carbon black on pyrolytic graphite	97.9	96.4	98.5	210
Textured pyrolytic gaphite	98.0	96.1	98.1	200
Pyrolytic graphite (*AB*-plane)	97.5	95.3	97.5	230
Copper	97.0	94.7	97.5	300

TABLE XIII.—AVERAGE TWT-T MEC 103 AND MDC 3 PERFORMANCE AT SATURATION ACROSS 4.8- TO 9.6- GHz OPERATING BAND WITH CARBON BLACK AND PYROLYTIC-GRAPHITE-MDC ELECTRODES

(a) $I_0 = 0.38$ A

Electrode surface characteristics	RF efficiency, percent	Overall efficiency, percent	MDC efficiency, percent
Carbon black	11.8	39.3	82.4
Pyrolytic graphite[a]	11.8	[b]37.3	81.1

(b) $I_0 = 0.40$ A

Carbon black	12.5	41.1	82.8
Pyrolytic graphite[a]	12.5	[a]39.0	81.1

(c) $I_0 = 0.42$ A

Carbon black	12.9	41.1	82.5
Pyrolytic graphite[a]	12.9	[b]39.9	80.9

[a]Mixture of *AB*-plane and *C*-direction.

[b]Adjusted individually (at each I_0) to reflect slightly higher TWT-body power during the pyrolytic-graphite-collector test as measured subsequently with an undepressed collector.

TABLE XIV.—COLLECTOR PERFORMANCE ANALYSIS WITH DC BEAM FOR 8- TO 18- GHz TWT's (ref. 11) AND GRAPHITE MDC'S

Electrode surface characteristics	η_{col} (limit), percent	η_{col} (meas.), percent	$\frac{\eta_{col}(\text{meas.})}{\eta_{col}(\text{limit})} \times 100$, percent	Incident energy, eV	$\frac{I_{e3}}{(I_0 - I_B)} \times 100$, percent	$\frac{I_s}{I_0} \times 100$, percent
Isotropic graphite	77.2	[a]77.1	99.9	2190	99.1	0.5
Textured pyrolytic graphite	78.2	[a]78.0	99.7	2100	99.1	.7
Pyrolytic graphite (*C*-direction)	74.2	[a]74.0	99.7	2475	98.5	.1

[a]Assume I_B = 1 mA (0.004 I_0).

1. Report No.	2. Government Accession No.	3. Recipient's Catalog No.
NASA TP-2622		

4. Title and Subtitle	5. Report Date
Secondary-Electron-Emission Losses in Multistage Depressed Collectors and Traveling-Wave-Tube Efficiency Improvements With Carbon Collector Electrode Surfaces	September 1986
	6. Performing Organization Code: 506-44-21
7. Author(s): Peter Ramins and Ben T. Ebihara	8. Performing Organization Report No.: E-3062
	10. Work Unit No.
9. Performing Organization Name and Address: National Aeronautics and Space Administration, Lewis Research Center, Cleveland, Ohio 44135	11. Contract or Grant No.
	13. Type of Report and Period Covered: Technical Paper
12. Sponsoring Agency Name and Address: National Aeronautics and Space Administration, Washington, D.C. 20546	14. Sponsoring Agency Code

15. Supplementary Notes

16. Abstract

An experimental program was conducted to investigate secondary-electron-emission losses in multistage depressed collectors (MDC's) and to determine their effects on the overall traveling-wave-tube (TWT) efficiency. Two representative TWT's and several computer-modeled MDC's were used. The experimental techniques provided the measurement of both the TWT overall and the collector efficiencies. The TWT-MDC performance was optimized and measured over a wide range of operating conditions, with geometrically identical collectors, which utilized different electrode surface materials. Comparisons of the performance of copper electrodes to that of various forms of carbon, including pyrolytic and isotropic graphites, were stressed. The results indicate that (1) a significant improvement in the TWT overall efficiency was obtained in all cases by the use of carbon, rather than copper electrodes, and (2) that the extent of this efficiency enhancement depended on the characteristics of the TWT, the TWT operating point, the MDC design, and the collector voltages. Ion textured graphite was found to be particularly effective in minimizing the secondary-electron-emission losses. Experimental and analytical results, however, indicate that it is at least as important to provide a maximum amount of electrostatic suppression of secondary electrons by proper MDC design. Such suppression, which is obtained by ensuring that a substantial suppressing electric field exists over the regions of the electrodes where most of the current is incident, was found to be very effective. Experimental results indicate that, with proper MDC design and the use of electrode surfaces with low secondary-electron yield, degradation of the collector efficiency can be limited to a few percent.

17. Key Words (Suggested by Author(s))	18. Distribution Statement
Traveling-wave tube, multistage depressed collector, graphite electrodes, secondary-electron emission	Unclassified - unlimited STAR Category 33

19. Security Classif. (of this report)	20. Security Classif. (of this page)	21. No. of pages	22. Price*
Unclassified	Unclassified	23	A02

*For sale by the National Technical Information Service, Springfield, Virginia 22161

NASA-Langley, 1986

National Aeronautics and
Space Administration
Code NIT-4

Washington, D.C.
20546-0001